Probing cis-trans isomerization in the S1 state of C2H2 via H-atom action and hot band-pumped IR-UV double resonance spectroscopies

Citation: Changala, P. Bryan, Joshua H. Baraban, Anthony J. Merer, and Robert W. Field. "Probing Cis-Trans Isomerization in the S1 State of C2H2 via H-Atom Action and Hot Band-Pumped IR-UV Double Resonance Spectroscopies." J. Chem. Phys. 143, no. 8 (August 28, 2015): 084310. © 2015 AIP Publishing LLC.

As Published: http://dx.doi.org/10.1063/1.4929588

Publisher: American Institute of Physics (AIP)

Persistent URL: http://hdl.handle.net/1721.1/106799

Version: Final published version: final published article, as it appeared in a journal, conference proceedings, or other formally published context

Probing cis-trans isomerization in the S1 state of C2H2 via H-atom action and hot band-pumped IR-UV double resonance spectroscopies

P. Bryan Changala, Joshua H. Baraban, Anthony J. Merer, and Robert W. Field

Citation: The Journal of Chemical Physics **143**, 084310 (2015); doi: 10.1063/1.4929588
View online: http://dx.doi.org/10.1063/1.4929588
View Table of Contents: http://scitation.aip.org/content/aip/journal/jcp/143/8?ver=pdfcov
Published by the AIP Publishing

Probing *cis-trans* isomerization in the S_1 state of C_2H_2 via H-atom action and hot band-pumped IR-UV double resonance spectroscopies

P. Bryan Changala,[1,a)] Joshua H. Baraban,[1,b)] Anthony J. Merer,[2,3] and Robert W. Field[1,c)]
[1]*Department of Chemistry, Massachusetts Institute of Technology, Cambridge, Massachusetts 02139, USA*
[2]*Institute of Atomic and Molecular Sciences, Academia Sinica, Taipei 10617, Taiwan*
[3]*Department of Chemistry, University of British Columbia, Vancouver, British Columbia V6T 1Z1, Canada*

(Received 7 July 2015; accepted 14 August 2015; published online 27 August 2015)

We report novel experimental strategies that should prove instrumental in extending the vibrational and rotational assignments of the S_1 state of acetylene, C_2H_2, in the region of the *cis-trans* isomerization barrier. At present, the assignments are essentially complete up to ~500 cm^{-1} below the barrier. Two difficulties arise when the assignments are continued to higher energies. One is that predissociation into $C_2H + H$ sets in roughly 1100 cm^{-1} below the barrier; the resulting quenching of laser-induced fluorescence (LIF) reduces its value for recording spectra in this region. The other difficulty is that tunneling through the barrier causes a staggering in the K-rotational structure of isomerizing vibrational levels. The assignment of these levels requires data for K values up to at least 3. Given the rotational selection rule $K' - \ell'' = \pm 1$, such data must be obtained via excited vibrational levels of the ground state with $\ell'' > 0$. In this paper, high resolution H-atom resonance-enhanced multiphoton ionization spectra are demonstrated to contain predissociated bands which are almost invisible in LIF spectra, while preliminary data using a hyperthermal pulsed nozzle show that $\ell'' = 2$ states can be selectively populated in a jet, giving access to $K' = 3$ states in IR-UV double resonance. © *2015 AIP Publishing LLC.* [http://dx.doi.org/10.1063/1.4929588]

I. INTRODUCTION

The spectroscopy of acetylene dates back more than a century to 1913,[1,2] though 40 years passed before the first successful analyses of the $\tilde{A}$–$\tilde{X}$ system were carried out by Ingold and King[3] and Innes.[4] The transition is now known to be a $\pi^* \leftarrow \pi$ excitation from the linear ground state to a *trans*-bent excited state, S_1 ($\tilde{A}^1A_u$). Further detailed analyses by Watson *et al.*,[5–7] the Crim group,[8,9] Yamakita and Tsuchiya,[10–12] and Merer *et al.*[13–17] have led to an essentially complete assignment of the vibrational and rotational structure up to 4500 cm^{-1} above the zero-point level of the $\tilde{A}$ state. One of the most interesting results of these analyses has been the discovery[17,18] of bands that belong to the *cis*-bent isomer of the $\tilde{A}$ state, the zero-point level of which lies about 2670 cm^{-1} higher in energy than that of the *trans*-bent isomer. The existence of the *cis* isomer had been predicted by several theoretical studies,[19–24] but it was thought that the $\tilde{A}$ state of the *cis* isomer would be unobservable because it transforms as $^1A_2$ in the C_{2v} point group; thus, transitions to it from the $^1\Sigma_g^+$ ground state are electric dipole forbidden. Recent calculations[25] place the barrier to *cis-trans* isomerization about 5000 cm^{-1} above the minimum energy of the *trans* isomer.

Starting about 500 cm^{-1} below the *cis-trans* barrier, the onset of isomerization causes the vibrational and rotational structure of the S_1 state to become very complicated. The levels of the bending vibrations, ν_4 (torsion, a_u) and ν_6 (*cis* bend, b_u) interact strongly by Darling-Dennison[26] and Coriolis resonances,[9] such that the vibrational structure of these modes forms polyads, which are groups of levels with the same value of $v_4 + v_6$. Their rotational structure is highly irregular,[9,14,16] though it can be modeled with an effective Hamiltonian. Simultaneous excitation of ν_3 (*trans* bend, a_g) progressively destroys the bending polyad structure[16] because the saddle point on the potential surface at the isomerization barrier results in very large anharmonicity in the 3^m6^n combination levels. The reason for this is that the pathway to the predicted[19–24] half-linear geometry at the saddle point is a CCH local bending motion formed from the combination of the normal coordinates Q_3 and Q_6. At the saddle point, the local bending vibrational intervals must go through a minimum, in similar fashion to the "Dixon dip"[27] of the large amplitude bending intervals in triatomic molecules. Recent calculations of the level structure near the barrier[25,28,29] support this conclusion.

Although the ν_3/ν_6 anharmonic interaction restores some of the regularity of the asymmetric top patterns, quantum mechanical tunneling through the barrier starts to disrupt the patterns in a different way. There are two effects. The first is a tunneling splitting between equivalent structures differing only in the bending angles at the two ends of the molecule. For group theoretical reasons,[30] this produces an even-odd staggering of the K-structure of a vibrational level. In addition, interactions occur between *cis* and *trans* levels at similar energies.[18,28,30] These are the mechanisms by which the *cis* levels obtain their intensity by mixing with nearby *trans* levels,

a)Current address: JILA, National Institute of Standards and Technology and Department of Physics, University of Colorado, Boulder, Colorado 80309, USA.
b)Current address: Department of Chemistry, University of Colorado, Boulder, Colorado 80309, USA.
c)Email: rwfield@mit.edu

though the selection rules and level shifts are different for even and odd K-values. Combining these two effects, the resulting K-staggering varies in a seemingly random fashion from level to level. If isomerization through the torsional vibration is important, as in H_2O_2, there will be a further staggering of the $K = 4n$ levels versus the $K = 4n + 2$ levels.[30] Preliminary results suggest that this further staggering is not significant,[28] but it is clear that full analyses of the K-structure require data from K values up to 3 or possibly 4.

Unfortunately, the S_1-S_0 rotational selection rule, $K' - \ell'' = \pm 1$, stands in the way. Jet cooling is essential to simplify the comparatively dense rotational structure, but it also reduces the vibrational temperature, so that most of the molecules are in the zero-point level of the linear ground state, where $\ell'' = 0$. Higher values of ℓ'' occur in the levels where the degenerate bending vibrations, ν_4'' and ν_5'', are excited, so that these levels must be populated if transitions to the higher K' levels of the upper state are to be observed. In this paper, we demonstrate the "proof of principle" that such lower state vibrational levels can be populated with the use of a pulsed hyperthermal nozzle, which raises the vibrational temperature while barely affecting the rotational temperature. With an IR laser, we have selectively excited molecules from the $2\nu_4''$ (Δ_g) level to the $\nu_3'' + 2\nu_4''$ (Δ_u) level, where $\ell'' = 2$, and then excited the molecules to the 3^36^1, $K' = 3$ level with an UV laser. The properties of the hyperthermal nozzle have also been investigated.

The isomerization barrier in the $\tilde{A}$ state lies about 1100 cm^{-1} above the predissociation limit for $C_2H_2 \rightarrow C_2H + H$, at 46 074 ± 8 cm^{-1}.[31] As many authors have found,[11,31–36] the diminishing fluorescence quantum yield at higher energies limits the usefulness of laser-induced fluorescence (LIF) for the recording of spectra. Instead, resonance-enhanced multi-photon ionization (REMPI) detection of H atoms has been shown[11,31–36] to be increasingly attractive for detection, since the absorption strength of the transition and the H atom yield both increase above the isomerization barrier. In the present paper, we demonstrate that REMPI spectra at higher resolution permit the observation, with good signal-to-noise, of a predissociated band that is barely observable with LIF detection.

II. EXPERIMENTAL DETAILS

A. H-atom action apparatus

The molecular beam source chamber of the H-atom REMPI experiments consisted of a vacuum chamber fitted with an oil diffusion pump (Varian, VHS-6), itself backed by a belt drive pump (Welch, 1397). The chamber contained a pulsed solenoid value (General Valve, Series 9, 1 mm orifice diameter), operated at 20 Hz. The source chamber reached an ultimate pressure of $<1 \times 10^{-6}$ Torr. Under load, pressures rose to $<1 \times 10^{-3}$ Torr. Mixtures of acetylene (10%-25%) in He or Ar were expanded with a backing pressure of 1-4 atm.

After exiting the pulsed valve, the gas expansion passed through a conical skimmer (~1 mm orifice diameter), placed approximately 5 cm downstream, into a second differentially pumped detection chamber. The detection chamber was pumped with a turbopump (Varian, V-250), and reached an ultimate pressure of $\sim 10^{-7}$ Torr, while remaining below 1×10^{-5} Torr under load. After the skimmer, the beam passed through velocity map imaging style ion optics,[37] consisting of a repeller, extractor, and ground plate, each spaced 1 in. apart. Halfway between the repeller and extractor plates, laser radiation (see below) was used to dissociate molecules in the beam and subsequently ionize the H-atom fragments. After continuing through a 9 in. field-free drift region, the molecular beam reached a MCP detector (Jordan TOF, C-701) where ionized fragments were measured. The output signal of the detector was monitored on a digital oscilloscope (LeCroy) and the data transferred to a personal computer (PC) for storage and post-processing. Weak signals were amplified with a fast preamplifier (Femto, DHPVA-200), which increased the dynamic range of the spectra.

Two lasers were required for the H-atom REMPI experiments, the first to excite an $\tilde{A}$–$\tilde{X}$ transition to a predissociated state, and the second to ionize the resulting H-atom fragment. The excitation beam was produced by a tunable dye laser (Lambda Physik, FL3002E) pumped by the third harmonic (355 nm) of a Q-switched, injection-seeded Nd:YAG laser (Spectra Physics, PRO-270), operating at 20 Hz. This dye laser was equipped with an intracavity etalon and operated around 420-430 nm (Stilbene 420 dye), yielding an output with ~0.04 cm^{-1} line width. This radiation was frequency doubled in a β-barium borate (BBO) crystal to produce UV radiation. Its frequency was calibrated by simultaneous measurement of $^{130}Te_2$ absorption ($\sigma = 0.02$ cm^{-1}) of the blue fundamental. The doubled UV light had a pulse energy of ~150 μJ. The REMPI laser radiation was produced with a second tunable dye laser (Sirah GmbH, Cobra-Stretch), pumped by a Nd:YAG laser, tuned to 20 564.74 cm^{-1} (linewidth of ~0.05 cm^{-1}). After doubling in a β-BBO crystal, the H-atom 2 + 1 REMPI frequency was generated with a pulse energy of ~500 μJ. Both the excitation and REMPI beams were routed to the detection chamber and focused with 50 and 30 cm focal length lenses, respectively, to interact with the skimmed molecular beam halfway between the repeller and extractor ion optic plates. The two beams were spatially and temporally overlapped. The REMPI laser beam was additionally retroreflected by an UV-enhanced aluminium spherical mirror (Thorlabs), which greatly enhanced the H-atom 2 + 1 REMPI signal. Under these conditions, it was also possible to observe 1 + 1 REMPI of C_2H_2 resulting from the focused excitation beam. The H-atom action spectrum was generated by gating on the appropriate TOF signal from the MCP detector.

B. Hot band-pumped IR-UV DR apparatus

The hot band-pumped IR-UV double resonance (DR) experiments were carried out within the source chamber of the apparatus just described. A hyperthermal pyrolysis microreactor nozzle, based on that used by the Ellison group,[38] replaced the standard pulsed valve. The hyperthermal nozzle consisted of a pulsed solenoid valve fitted with a SiC tube (1 mm ID, 2 mm OD, ~4 cm long) heated by passing a current through it, thus achieving temperatures up to 1800 K. (Note that a constant current source, rather than a constant voltage source, had to be used to heat the tube stably due

to the anomalous temperature dependence of SiC resistivity.) Mixtures of acetylene (10%-25% in He) were expanded through the nozzle with a backing pressure of 4 atm.

The IR radiation used to pump hot band transitions within the ground electronic state of acetylene was generated from a third tunable dye laser (Lambda Physik, FL2002) pumped by the second harmonic (532 nm) of a Nd:YAG laser. Wavelengths around 790 nm were produced (LDS 798 dye) and subsequently mixed with the Nd:YAG fundamental (1064 nm) in a $LiNbO_3$ crystal (Spectra Physics, WEX) to generate 3 μm IR radiation via difference frequency generation. The IR radiation was further amplified in a second $LiNbO_3$ optical parametric amplifier (OPA) crystal pumped by 1064 nm light, yielding a pulse energy of 1.5 mJ. The IR output had a spectral width of 0.15 cm^{-1}. The IR wavelength was calibrated by photoacoustic measurements of known C_2H_2 cold band transitions in a static gas cell at room temperature.

The UV radiation was generated with the same equipment as the REMPI laser above. Both the IR and UV radiation (unfocused) were routed to the molecular beam source chamber, where they interacted with the unskimmed gas expansion 2 cm downstream from the end of the SiC nozzle. The UV pulse was delayed 100 ns after the IR pulse. Laser induced fluorescence was detected perpendicularly to both the gas expansion and the laser beams with a head-on photomultiplier tube (PMT) (Hamamatsu, R375) and $f/1.2$ collection optics. The PMT input was filtered with a dichroic mirror (ArF 45° HR @ 193 nm) and colored glass filters (UG-5 or UG-11) to reduce laser scatter. Additionally, the laser window arms of the source chamber were equipped with 4 iris baffles, which further reduced laser scatter. The PMT signal was acquired on a digital oscilloscope (LeCroy) and stored on a PC for post-processing. As above, weak signals were amplified with a fast preamplifier to extend the measurable dynamic range.

III. RESULTS AND DISCUSSION

A. H-atom action spectra

We have recorded high resolution H-atom action spectra from the 46 250-47 250 cm^{-1} region (corresponding to 4000-5000 cm^{-1} above the *trans* origin). These new data have a spectral resolution about 5× better than previous H-atom action spectra of the $\tilde{A}$–$\tilde{X}$ system.[11,36] One particularly important early finding is shown in Figure 1, which shows a hot band going to the $K' = 2$ level of the *trans*-$3^4 6^2$ vibrational state. The band is much more prominent in the H-atom action spectrum than in the corresponding LIF spectrum, where overlapping features mostly obscure it. Combining the position of this $K' = 2$ state (47 268 cm^{-1}) with those of the $3^4 6^2$ $K' = 0$ and $K' = 1$ states (47 195 and 47 206 cm^{-1}, respectively), we calculate an apparent K-staggering of −6.9 cm^{-1}. In addition to providing information on the extent of isomerization tunneling and *cis-trans* interactions, this measurement is necessary to deperturb the input data for effective frequency dip analyses, which can provide a detailed characterization of the isomerization transition state.[29]

It is interesting to compare this staggering to that of other *trans* levels in the ν_6 progression. 3^4 has a staggering of 0 cm^{-1}

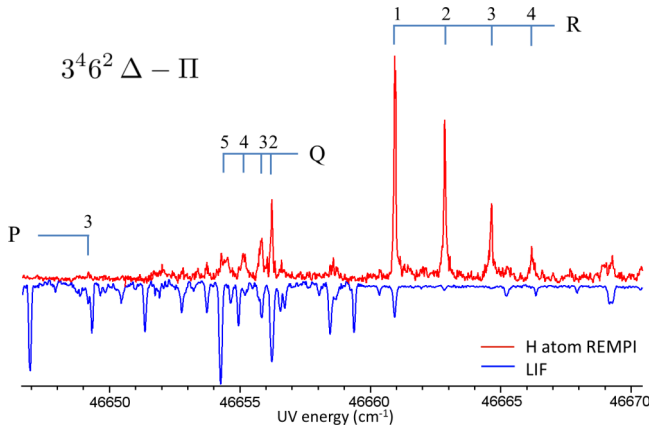

FIG. 1. H-atom action (red, upper trace) and our unpublished LIF (blue, lower trace) spectra of $3^4 6^2$ $K = 2$. This hot band originates from the ν_4'' ($\ell'' = 1$) level; the change in angular momentum upon excitation is denoted by the Greek symbols in the upper left of the figure. UV excitation energy is given in cm^{-1}. J'' assignments are shown by the tie-lines. The relative strength of the $3^4 6^2$ band compared to overlapping features is much higher in the H-atom REMPI spectrum than the LIF spectrum due to significant predissociation. Overlapping features, not labeled in the spectra, include transitions to $2^1 3^3$ (both ^{12}C and possibly ^{13}C isotope lines), $1^1 6^2$, and the $3^3 B^2$ polyad.[6,16]

to within fit uncertainties and $3^4 6^1$ has an apparent staggering of about +27 cm^{-1}. It is perhaps surprising that the staggering in $3^4 6^2$ is *smaller* in magnitude than that of $3^4 6^1$. $3^4 6^2$ is naively expected to be more "isomerization active" (as it is the combination of ν_3 and ν_6 that follows the isomerization path), so that one would expect it to exhibit a larger tunneling staggering. Indeed, reduced dimension *ab initio* calculations predict an increasing staggering magnitude along the $3^4 6^{0-2}$ progression.[28] This discrepancy is not understood. Misassignment is a possibility, though in the present case it seems unlikely. We speculate that it may instead be due to sensitive interactions between levels in the nonequivalent *cis* and *trans* wells. While simple tunneling trends might be expected for highly symmetric systems, such as ammonia inversion or methyl rotors, the zero-order vibrational level patterns of the *cis* and *trans* wells are essentially independent of each other. Thus, local K-dependent *cis-trans* interactions yield patterns that are difficult to predict and spectra that are difficult to interpret. Small changes in relative level positions can yield qualitative changes in tunneling and staggering patterns. Further measurements of isomerizing levels, such as $3^4 6^2$, provided by H-atom REMPI detection are necessary to sort out these complications.

B. Demonstration of hot band enhancement

As the primary purpose of the hyperthermal nozzle described above is to populate vibrationally excited states, we first present a quantitative characterization of the state distribution of the molecular beam output. The main quantity of interest is the vibrational population enhancement factor for each vibrational level, defined as the relative population increase in the heated molecular beam versus an unheated beam. The population enhancement curves for the vibrational levels $v_4'' = \ell'' = 0$–3 of the electronic ground state are shown

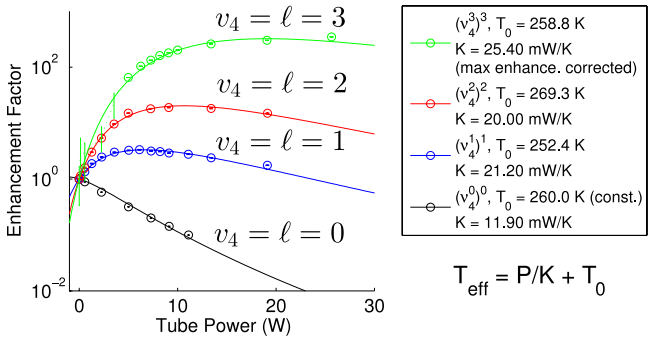

FIG. 2. Population enhancement of vibrational levels versus hyperthermal nozzle tube power. The enhancement factors, defined in Eq. (4), for $v_4 = \ell = 0$–3 are plotted (double primes omitted). A crude dissipative temperature model that relates the effective temperature of the tube to the tube power ($T_{\text{eff}} = P/K + T_0$), was used to generate fit curves. The enhancement factor curve for each vibrational level was fit separately. These data were measured for 10% mixtures of C_2H_2 in He (4 atm total backing pressure). For the $v_4 = \ell = 3$ data, low tube power LIF signals were very weak; the relative enhancement factors were rescaled such that the max enhancement factor (that of the highest tube power data point) was constrained to be 350. For the $v_4 = \ell = 0$ fit, the T_0 parameter was found to be poorly determined, and so was held constant at 260.0 K during the fit.

in Figure 2. The enhancement factors were measured by monitoring the LIF signal of one-photon $\tilde{A}$–$\tilde{X}$ transitions that originate from each vibrational state as the SiC tube power was gradually increased. Measurements of the rotational distribution at elevated tube temperatures confirm that the rotational temperature of the gas expansion remains cold (~10 K), so that measured signal enhancements could be attributed only to changes in the vibrational level populations.

Figure 2 also shows fits to a simple model of the thermal behavior of the gas in the tube. The model assumes that the vibrational populations conform to a quasi-Boltzmann distribution

$$P_i(T_{\text{eff}}) = \frac{\exp(-E_i/k_B T_{\text{eff}})}{Q_{\text{vib}}(T_{\text{eff}})}, \tag{1}$$

where P_i is the population of level i, which has term energy E_i, and Q_{vib} is the vibrational partition function. The effective temperature, T_{eff}, depends on the tube power and dissipative processes in the hyperthermal nozzle.

We approximate the vibrational partition function as that of a set of independent harmonic oscillators

$$Q_{\text{vib}}(T) \approx \prod_{i=1}^{5} \left(\frac{1}{1 - \exp(-\nu_i/k_B T)} \right)^{g_i}, \tag{2}$$

where ν_i and g_i are the frequency and degeneracy, respectively, of mode i (modes ν_4'' and ν_5'' have $g = 2$). We estimate that the error of this partition function over the energy regions of interest ($E_{\text{vib}} < 2000\ \text{cm}^{-1}$) is smaller than that introduced by other approximations made in this model.

As we have no direct temperature measurement of the heated tube, we determine an effective temperature by assuming the following: (i) the tube is heated solely by the resistive heating caused by the current passed through it, such that the input power is $P = IV$, where I and V are the (known) supplied current and voltage and (ii) the nozzle dissipates heat to a thermal bath at temperature T_0 with a dissipation constant of K, such that the power dissipated is $K(T - T_0)$. The steady-state temperature of this system is

$$T_{\text{steady}} \equiv T_{\text{eff}} = \frac{P}{K} + T_0. \tag{3}$$

The vibrational enhancement factor, ε, for level i is thus

$$\varepsilon_i(T_{\text{eff}}) = P_i(T_{\text{eff}})/P_i(T_0). \tag{4}$$

The values of T_0 and K are fit parameters, which are determined via a non-linear least-squares fit. The right panel of Figure 2 shows the values of these parameters for each vibrational level population enhancement curve. The T_0 values, in particular, are quite reasonable when compared to the effective vibrational temperature of C_2H_2 expanded in a 20% He mixture, which was measured to be 240 ± 20 K by Suzuki and Hashimoto.[36] Performing a separate fit for each vibrational level worked better than a simultaneous, global fit, especially for the $v_4'' = \ell'' = 0$ curve, which has a K parameter roughly 1/2 the magnitude of the other fits. Doubling the value of K to ~20 mW/K for this fit would scale the curve horizontally by the same amount and would clearly not reproduce the observed enhancement factors.

Our model is relatively crude, and more sophisticated treatments are called for to accurately model the non-trivial vibrational excitation processes occurring in the hyperthermal nozzle. However, our analysis demonstrates that the vibrational populations behave qualitatively as expected. The ground state is increasingly depleted as the tube temperature is increased. This population is redistributed to higher lying vibrational levels. The enhancement factors of the lower energy levels peak at lower temperatures, before their populations are in turn depleted by increasing temperature. Higher energy states have larger maximum enhancement factors, as their initial population without heating is correspondingly lower. Population enhancements of $>10^2$ for high ℓ'' states can easily be achieved, greatly facilitating the acquisition of hot band-pumped IR-UV DR spectra.

C. Hot band-pumped IR-UV double resonance: Proof of principle

Our first demonstration of a hot band-pumped IR-UV double resonance spectrum of S_1 acetylene is shown in Figure 3. The spectrum contains the Q(3) and R(3) lines of the 3^36^1, $K' = 3 \leftarrow \nu_3'' + 2\nu_4''$, $\ell'' = 2$ band. J-selectivity can be achieved by pumping a single rotational transition of the IR hot band (in this case R(2) of the $\nu_3'' + 2\nu_4''$, $\ell'' = 2 \leftarrow 2\nu_4''$, $\ell'' = 2$ band). Although the rotational cooling of the gas expansion prevents an overly crowded spectrum, the much wider vibrational population distribution in the heated jet results in numerous one-photon UV hot band transitions that would not appear in vibrationally colder spectra. These unwanted lines can be identified at once because they are present in spectra taken without the IR pump.

From Figure 2, it can be seen that the maximum $2\nu_4''$ population enhancement is about 20×. Without this enhancement, the hot band-pumped IR-UV transitions to 3^36^1 $K' = 3$ would be almost unobservable. (The signal-to-noise ratio here is approximately 30.) The assignment

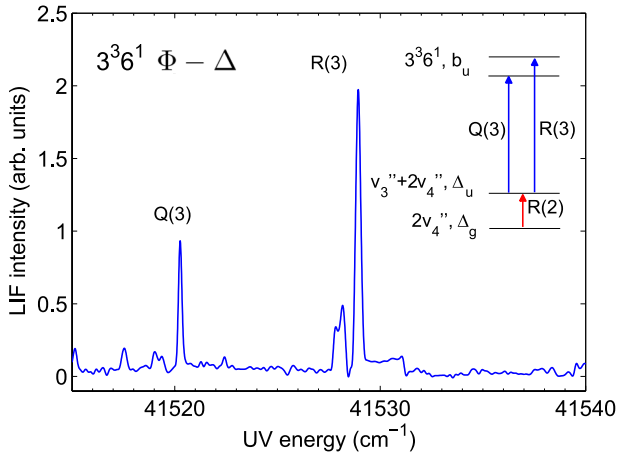

FIG. 3. Hot band-pumped IR-UV double resonance LIF spectrum of 3^36^1 $K' = 3$. The UV excitation energy is plotted in cm^{-1}. The excitation scheme is shown in the diagram on right, with vibrational symmetries. The Greek symbols denote angular momentum. The R(2) line of the $\nu_3'' + 2\nu_4'' \leftarrow 2\nu_4''$ band is IR pumped, populating the intermediate $J = 3$ level. The resulting Q(3) and R(3) lines of the UV band are shown. The unassigned lines in this spectrum correspond to 1-photon hot band transitions resulting from the ~800 K effective vibrational temperature.

of these transitions is easily verified as this $K' = 3$ level has been previously observed in IR-UV DR spectra via the $\nu_3'' + \nu_4''(\ell'' = 1)$ level, where it gains intensity only through strong Coriolis coupling to the $K' = 1$ level.

High K' data of S_1 vibrational levels, such as this $K' = 3$ level, are critical to assessing possible tunneling staggerings of isomerizing levels. Such an analysis of the 3^36^1 vibrational level is complicated by the fact that this level is Coriolis coupled to its polyad partner, 3^34^1, and suffers additional local perturbations.[10,17] Such perturbations obscure the K-staggering patterns that we observe more clearly in other isomerizing levels, such as *cis* 3^16^1 or *cis* 6^2, that do not exhibit complications from Coriolis or Darling-Dennison interactions. However, with a sufficient number of observed K levels, it is possible to determine staggering parameters, even in highly distorted polyads, via effective Hamiltonian models. The extended K observations made possible by hot band-pumped IR-UV DR spectra are essential to the success of such approaches and should play an important role in ongoing and future analyses of the near-barrier region.

IV. CONCLUSION

The ongoing study of *cis-trans* isomerization and its effect on the rovibrational level structure of S_1 C_2H_2 require continuous adaptation of spectroscopic techniques. The simultaneous problems of detection and state preparation, both of which worsen as the barrier to isomerization is approached, have been addressed by improved sensitivity H-atom action and hot band-pumped IR-UV double resonance spectroscopies, respectively. The preliminary results presented here demonstrate the effectiveness of such techniques. Future H-atom action and hot band-pumped IR-UV DR spectra will provide new and necessary information that will enable continued progress in our understanding of the near- and above-barrier dynamics of S_1 *cis-trans* isomerization.

ACKNOWLEDGMENTS

This work was supported by a grant from the U.S. Department of Energy (Grant No. DE-FG0287ER13671). A.J.M. thanks Academia Sinica (Taiwan) for a Distinguished Visiting Professorship, and the Natural Sciences and Engineering Research Council of Canada for some travel funds. The authors also wish to thank Arthur Suits and Bernadette Broderick for their advice and expertise in constructing the H-atom REMPI apparatus.

[1]V. Henri and M. Landau, Comptes Rendus **156**, 697 (1913).
[2]J. Stark and P. Lipp, Z. Phys. Chem. **86**, 36 (1913).
[3]C. K. Ingold and G. W. King, J. Chem. Soc. **1953**, 2702.
[4]K. K. Innes, J. Chem. Phys. **22**, 863 (1954).
[5]J. K. G. Watson, M. Herman, J. C. Van Craen, and R. Colin, J. Mol. Spectrosc. **95**, 101 (1982).
[6]J. C. Van Craen, M. Herman, R. Colin, and J. K. G. Watson, J. Mol. Spectrosc. **111**, 185 (1985).
[7]J. C. Van Craen, M. Herman, R. Colin, and J. K. G. Watson, J. Mol. Spectrosc. **119**, 137 (1986).
[8]J. D. Tobiason, A. L. Utz, and F. F. Crim, J. Chem. Phys. **99**, 928 (1993).
[9]A. L. Utz, J. D. Tobiason, E. Carrasquillo M., L. J. Sanders, and F. F. Crim, J. Chem. Phys. **98**, 2742 (1993).
[10]M. Mizoguchi, N. Yamakita, S. Tsuchiya, A. Iwasaki, K. Hoshina, and K. Yamanouchi, J. Phys. Chem. A **104**, 10212 (2000).
[11]N. Yamakita, S. Iwamoto, and S. Tsuchiya, J. Phys. Chem. A **107**, 2597 (2003).
[12]N. Yamakita and S. Tsuchiya, Chem. Phys. Lett. **348**, 53 (2001).
[13]A. J. Merer, N. Yamakita, S. Tsuchiya, J. F. Stanton, Z. Duan, and R. W. Field, Mol. Phys. **101**, 663 (2003).
[14]A. J. Merer, N. Yamakita, S. Tsuchiya, A. H. Steeves, H. A. Bechtel, and R. W. Field, J. Chem. Phys. **129**, 054304 (2008).
[15]A. H. Steeves, A. J. Merer, H. A. Bechtel, A. R. Beck, and R. W. Field, Mol. Phys. **106**, 1867 (2008).
[16]A. H. Steeves, H. A. Bechtel, A. J. Merer, N. Yamakita, S. Tsuchiya, and R. W. Field, J. Mol. Spectrosc. **256**, 256 (2009).
[17]J. H. Baraban, P. B. Changala, A. J. Merer, A. H. Steeves, H. A. Bechtel, and R. W. Field, Mol. Phys. **110**, 2707 (2012).
[18]A. J. Merer, A. H. Steeves, J. H. Baraban, H. A. Bechtel, and R. W. Field, J. Chem. Phys. **134**, 244310 (2011).
[19]H. Lischka and A. Karpfen, Chem. Phys. **102**, 77 (1986).
[20]J. F. Stanton, C.-M. Huang, and P. G. Szalay, J. Chem. Phys. **101**, 356 (1994).
[21]C. D. Sherrill, G. Vacek, Y. Yamaguchi, H. F. Schaefer, J. F. Stanton, and J. Gauss, J. Chem. Phys. **104**, 8507 (1996).
[22]K. Malsch, R. Rebentisch, P. Swiderek, and G. Hohlneicher, Theor. Chem. Acc. **100**, 171 (1998).
[23]E. Ventura, M. Dallos, and H. Lischka, J. Chem. Phys. **118**, 1702 (2003).
[24]B. Schubert, H. Köppel, and H. Lischka, J. Chem. Phys. **122**, 184312 (2005).
[25]J. H. Baraban, A. R. Beck, A. H. Steeves, J. F. Stanton, and R. W. Field, J. Chem. Phys. **134**, 244311 (2011).
[26]B. T. Darling and D. M. Dennison, Phys. Rev. **57**, 128 (1940).
[27]R. N. Dixon, Trans. Faraday Soc. **60**, 1363 (1964).
[28]P. B. Changala, J. H. Baraban, A. J. Merer, J. F. Stanton, and R. W. Field, J. Chem. Phys. **140**, 024313 (2014).
[29]J. H. Baraban, P. B. Changala, G. C. Mellau, J. F. Stanton, A. J. Merer, and R. W. Field, "Spectroscopic characterization of transition states" (to be published).
[30]J. T. Hougen and A. J. Merer, J. Mol. Spectrosc. **267**, 200 (2011).
[31]D. H. Mordaunt, M. N. R. Ashfold, R. N. Dixon, P. Löffler, L. Schnieder, and K. H. Welge, J. Chem. Phys. **108**, 519 (1998).
[32]M. Fujii, A. Haijima, and M. Ito, Chem. Phys. Lett. **150**, 380 (1988).
[33]A. Haijima, M. Fujii, and M. Ito, J. Chem. Phys. **92**, 959 (1990).
[34]N. Hashimoto and T. Suzuki, J. Chem. Phys. **104**, 6070 (1996).
[35]N. Hashimoto, N. Yonekura, and T. Suzuki, Chem. Phys. Lett. **264**, 545 (1997).
[36]T. Suzuki and N. Hashimoto, J. Chem. Phys. **110**, 2042 (1999).
[37]A. T. J. B. Eppink and D. H. Parker, Rev. Sci. Instrum. **68**, 3477 (1997).
[38]X. Zhang, A. V. Friderichsen, S. Nandi, G. B. Ellison, D. E. David, J. T. McKinnon, T. G. Lindeman, D. C. Dayton, and M. R. Nimlos, Rev. Sci. Instrum. **74**, 3077 (2003).